

## Review Article

Andreas Heinrich<sup>a,\*</sup>, Manuel Rank<sup>a</sup>, Philippe Maillard<sup>a</sup>, Anne Suckow<sup>a</sup>, Yannick Bauckhage<sup>a</sup>, Patrick Rößler<sup>a</sup>, Johannes Lang<sup>a</sup>, Fatin Shariff<sup>a</sup> and Sven Pekrul<sup>a</sup>

# Additive manufacturing of optical components

DOI 10.1515/aot-2016-0021

Received April 11, 2016; accepted May 20, 2016; previously published online June 25, 2016

**Abstract:** The development of additive manufacturing methods has enlarged rapidly in recent years. Thereby, the work mainly focuses on the realization of mechanical components, but the additive manufacturing technology offers a high potential in the field of optics as well. Owing to new design possibilities, completely new solutions are possible. This article briefly reviews and compares the most important additive manufacturing methods for polymer optics. Additionally, it points out the characteristics of additive manufactured polymer optics. Thereby, surface quality is of crucial importance. In order to improve it, appropriate post-processing steps are necessary (e.g. robot polishing or coating), which will be discussed. An essential part of this paper deals with various additive manufactured optical components and their use, especially in optical systems for shape metrology (e.g. borehole sensor, tilt sensor, freeform surface sensor, fisheye lens). The examples should demonstrate the potentials and limitations of optical components produced by additive manufacturing.

**Keywords:** additive manufacturing; materials; optical design and fabrication; polymers.

**OCIS codes:** 220.0220; 160.0160; 160.5470.

---

<sup>a</sup>The authors are all members of the optical metrology group at the Center for Optical Technologies at Aalen University. Since 2013, the focus of the group is on the additive manufacturing of optical components – transmissive optics, as well as reflective optics. The aim of the group is to find new solutions in the field of optical metrology and lighting through new design approaches, which are possible due to the additive manufacturing.

**\*Corresponding author: Andreas Heinrich**, Center for Optical Technologies, Aalen University, Anton Huber Straße 21, 73430 Aalen, Germany, e-mail: [Andreas.Heinrich@hs-aalen.de](mailto:Andreas.Heinrich@hs-aalen.de)  
**Manuel Rank, Philippe Maillard, Anne Suckow, Yannick Bauckhage, Patrick Rößler, Johannes Lang, Fatin Shariff and Sven Pekrul:** Center for Optical Technologies, Aalen University, Anton Huber Straße 21, 73430 Aalen, Germany

---

[www.degruyter.com/aot](http://www.degruyter.com/aot)

© 2016 THOSS Media and De Gruyter

## 1 Introduction

Additive manufacturing differentiate to ‘conventional’ production techniques due to the fact that material is added instead of removed. Therefore, different technologies were developed, especially in order to manufacture mechanical parts. Since several years, this production technique expands to new application fields like the manufacturing of optics in research and industry (e.g. [www.luxexcel.com/](http://www.luxexcel.com/); [www.formlabs.com](http://www.formlabs.com)).

A classification of the existing additive manufacturing methods would be according to the material used. Thereafter, one can distinguish between metallic materials and polymers. With respect to optical applications, this means a distinction between reflective and transmissive optics. In the case of reflective optics, materials like aluminum are used. A quite common additive manufacturing method for this material is selective laser melting (SLM) [1, 2]. The additive manufacturing of glass would have the advantage of a transparent material being used, but it may not allow sufficiently small structures [3]. In this work, we focus on the use of polymers. Structures in some 10-nm range can be created using two-photon polymerization or direct laser writing ([www.lightfab.de](http://www.lightfab.de)) [4]. Unfortunately, this is accompanied by a small sample size. Larger samples can be realized by means of the so-called ‘3D printers’. Common additive manufacturing methods are, in this case, fused deposition modeling (FDM), multi-jet modeling (MJM), or stereolithography (SLA) [5]. There are other methods such as printing of silicone [6] or additive manufacturing based on a powder method [7]. However, these methods are not considered here.

The FDM method is based on the melting of one or more plastic threads using one or more extrusion heads, which are movable. A 3D model is realized by a layered deposition of the material. Typical layer thicknesses are approximately 100  $\mu\text{m}$ . Thereby, the achievable minimal layer thickness depends on the print volume and the actuators used. For applications in the field of optics, this technique leads to inhomogeneous components, resulting in an extensive volume scattering of the light. Furthermore, the surface quality is quite poor in this process.

The MJM method is comparable to inkjet printing. Here, a liquid, UV-reactive resin is directly applied using a printhead. After a deposition of a thin layer, the material is leveled with a roller and cured with UV light. The minimum layer thicknesses that can be achieved with this technique are a few 10  $\mu\text{m}$ . In order to realize an overhanging structure, a second material (support material) is printed first, as an underlay material for the building material. The support material can be removed after the building process, e.g. by water or other chemical solvents.

In the case of the SLA method, resins are used as well. Again, they are applied in thin layers and cured afterward utilizing either a laser or by imaging UV light onto the resin using a DMD projector. The minimum achievable layer thicknesses are down to 5  $\mu\text{m}$ . In order to realize overhanging structures, the building material is also used as a support material. However, the generation of the support structure takes place as a filigree structure, which connects via predetermined breaking points to the building material. Unfortunately, this results in rough surfaces after the removal of the supporting structure.

The general workflow for the additive manufacturing of optical elements is the generation of the optical element in the optical design software with the required functionality, the export of the designed optics as ‘STL file’, which can be sent directly to the printer. The printer software ‘slices’ the model into thin layers, which are printed one after the other. As this is a completely different workflow offering a higher degree of freedom compared to the standard manufacturing methods of optical components, different design approaches are possible and needed. Thus, new optical designs and optical functionalities are possible like optically active substructures incorporated into monolithic optics.

## 2 Basic properties of additive manufactured components

For printing overhanging structures, a support material is necessary onto which the building material can be established. This is demonstrated for a sphere in Figure 1A. The bottom side of the sphere has to be supported by the yellow-marked material in order to be printed. Above the equator of the sphere, the building material, itself, acts as a support structure. The consequence of this is that one gets different surface characteristics. This can be seen in Figure 1B (SLA printed sphere). Thereby, ‘bottom

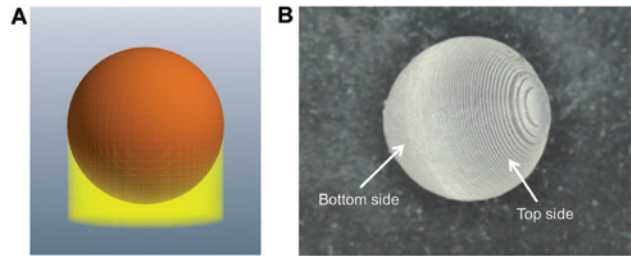


**Figure 1:** (A) Schematic model (orange: building material (sphere); yellow: support material). (B) Printed sphere (SLA process). Bottom side: part of the sphere that was surrounded by supporting material during printing.

side’ refers to the surface that is surrounded by support material. One can see a rough and unstructured surface. In comparison, the surface of the ‘top side’ of the sphere exhibits a layered structure due to the printing process. Typical layer thicknesses are 60–80  $\mu\text{m}$ . This step-like structure is needed in order to approximate the curvature of the sphere. Regardless of which side of the sphere is considered – in both cases, a rework is necessary to achieve a sufficient optical quality of the surface.

For optical applications, the transparency of the materials is crucial. As in the SLA process and in the case of the MJM process, polymers are used and cured with UV light (e.g. 405 nm or 365 nm), these materials do show a correspondingly high absorption in this wavelength range. Figure 2A shows the wavelength-dependent transmission of a typical MJM material (Keyence Agilista, Osaka, Japan; thickness of the sample: 10 mm). It indicates a clear decline in transmission below a wavelength of 425 nm, which is due to the necessary absorption described above. A printed optical component based on this material is presented in Figure 2B–D. Figure 2B shows the sample directly after printing. A strong orange color can be realized. In order to achieve a higher transparency of the sample, the sample was annealed at 100°C for 10 min (Figure 2C), 20 min (Figure 2D), and 30 min (Figure 2E). Already, visually, one can realize a significant improvement of the transmission. However, this method may influence the glass transition temperature of the material. Samples do improve slowly even without post-annealing. After several weeks without any treatment but regular ambient light, one can get the same result. It should be noted that the treatment method is dependent on the printing process and the printing material. In the case of SLA samples (Viper/3D Systems, SC, USA), a UV treatment significantly increases the transmission values. However, these samples have a negative long-term effect. They may get yellowish after a certain time. Ultimately, it is necessary to develop an individual post-treatment process for each material.

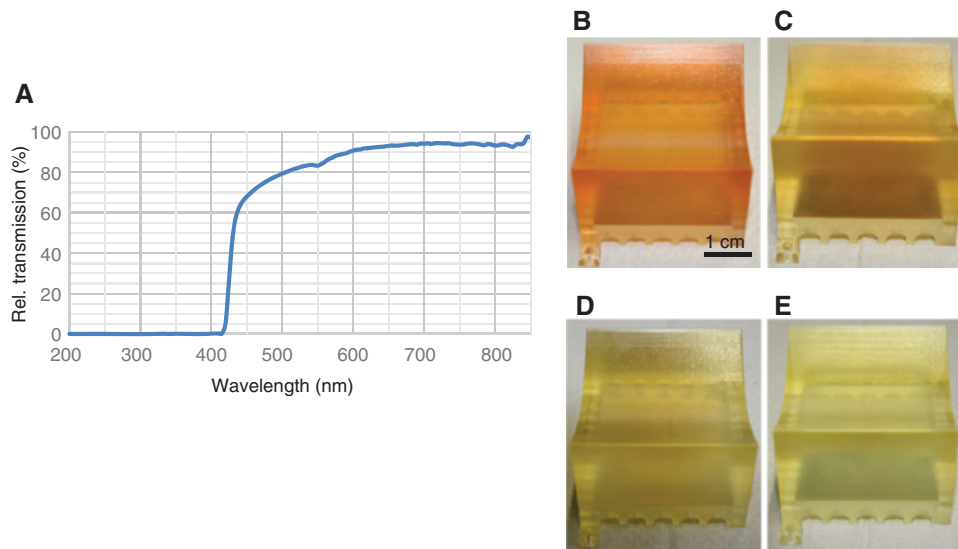


**Figure 2:** (A) Wavelength-dependent transmission (Keyence Agilista), (B) sample directly after printing, (C–D) sample after different annealing processes.

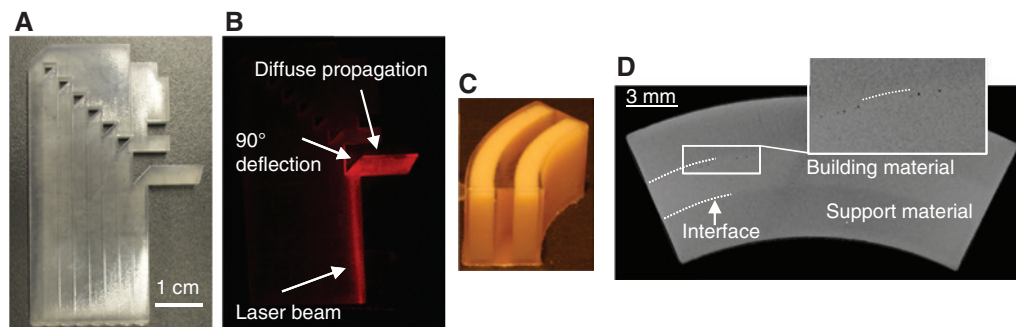


**Figure 3:** (A) Light pipe system (SLA process). (B) Propagation of a laser beam through one of the pipes. (C) Light pipe surrounded with support material (MJM process). (D) CT image of the inner structure.

Another important issue for 3d printed optics is the volume scattering of light in the material. In Figure 3A, a 3d-printed light pipe system is shown (SLA process). Light is coupled into the pipes (from below) and redirected to the right by total internal reflection at the trimmed surface. Figure 3B shows the transmission of a laser beam through one of the light pipes. Before the total reflection takes place, the laser beam can be clearly seen in the material. Thus, a substantial volume scattering is present. Certainly, a reason for this is the deposition of individual layers, whereby inhomogeneous material interfaces develop. In addition, in Figure 3B one can see diffuse light propagation after the reflection of the laser beam. This underlines the inadequate surface quality right after printing. Significant light scattering can be observed not only for samples prepared by the SLA process. MJM parts exhibit additionally air inclusions mainly at the interface building material/support material. This is demonstrated

in Figure 3C (curved light pipe). The bright material corresponds to the support material. The building material (material between the two bright areas) represents the light pipe. In order to analyze the internal structure of the component, a computer tomography was carried out (Figure 3D – position of the slice: around 1 mm from top of the part). It turned out that especially in the transition area between the two materials (see inset in Figure 3D), holes with a size of up to  $70\ \mu\text{m}$  exist. This might be due to the fact that support material and building material has to be printed for one single layer in parallel by two different printing heads. Certainly, these holes act as significant scattering centers as well.

Another important question concerning suitability and endurance of the material is the thermal stability of additive manufactured optics. This question arises especially when 3d-printed light-guiding optics is used for high-power applications. Figure 4A shows a light-guiding

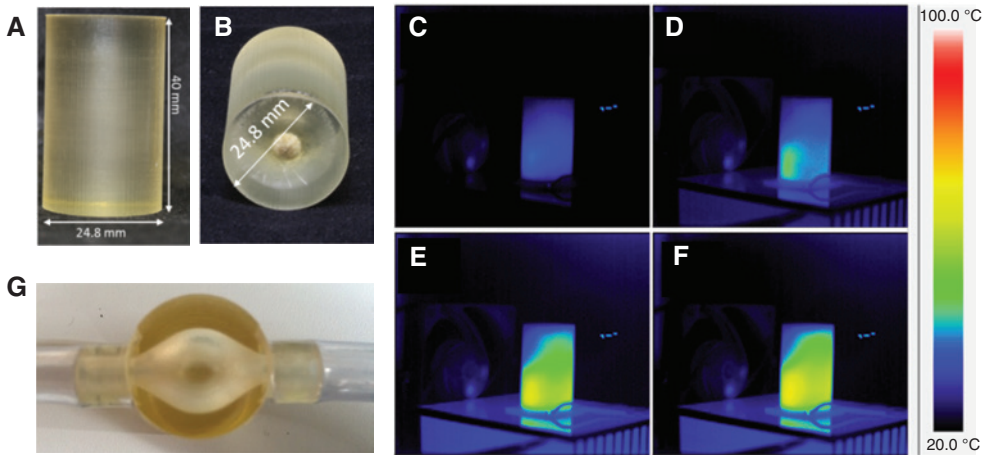


Figure 4: Studies on the thermal durability of additive manufactured optics.

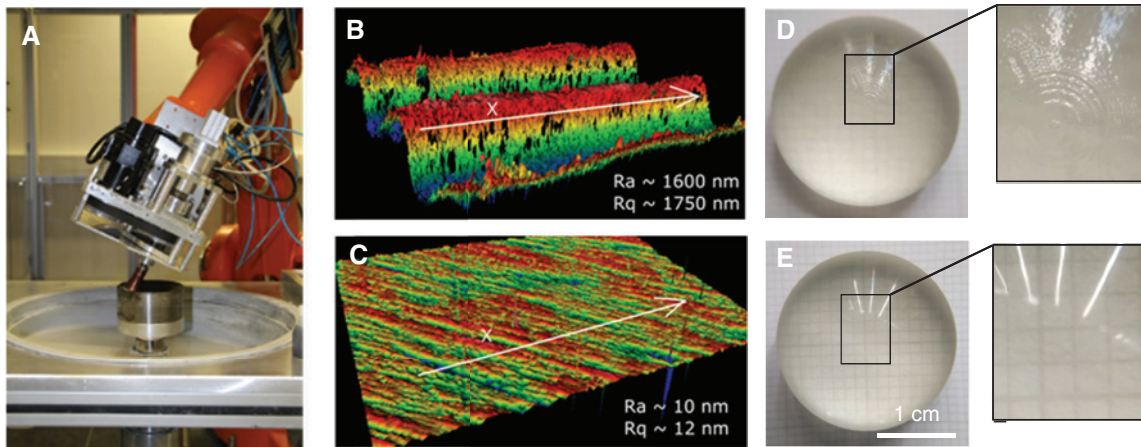


Figure 5: Rework of additive manufactured optical components. (A) Robot-based polishing system; (B) surface structure of an untreated sample; (C) surface structure of a robot-polished sample; (D) visual inspection of an untreated sample; (E) visual inspection of a coated sample.

rod (MJM method), which was implemented onto a high power LED (Cree CXA3070, NC, USA). With the help of an infrared camera, thermal imaging was carried out at 0 min and after 3 min, 7 min, and 10 min of operation (Figure 4C–F) (electrical power LED: 52 W). As can be seen in the figures, the material is heated in the lower region of the cylinder in the interior to about 90°C. It should also be noted that due to the poor thermal conductivity of the material, heat is hardly dissipated, thus, resulting in an accumulation of the heat. After 10 min, the temperature reached is above the glass transition temperature of the material (80°C), which leads to destruction in the interior of the printed optics (see Figure 4B). Active cooling of the optics is, therefore, essential for such applications. An advantage of additive manufacturing is that the necessary mechanical designs can be integrated directly into the optics. Figure 4G shows such a solution. In the lower area of the light pipe, a bubble-shaped cavity has been integrated into the volume of the light pipe. Cooling liquid can

be guided via the two mechanical connections. The refractive index of the cooling medium should be adapted to the polymer, so that there is no major impact on the light guiding. As a liquid cooling medium is used, the intrinsic roughness of the cavity in the light pipe is not an issue.

### 3 Post-processing of additive manufactured optics

As discussed in Chapter 3, additive manufactured components exhibit a rough surface. In Figure 5B, a white light interferometer measurement of the surface of an untreated printed sample is shown. The layered structure (thickness approximately 50 μm) can be recognized by the sine-shaped surface. Along the line drawn in Figure 5B, a surface roughness of  $R_a = 1.6 \mu\text{m}$  was determined. Thus, the components are not usable for optical applications,

and the surface need to be reworked. Optimal results are achieved when using robot-based polishing methods (see Figure 5A). A six-axis robot moves the polishing tool on the optical surface in accordance with a pre-programmed path. In a parallel liquid, polishing material is added. Finally, a surface like that shown in Figure 5C is reached (typical processing time: from some hours up to some days – depending on the complexity of the shape). The layered structure is no longer present, and the surface quality has significantly improved ( $R_a=10$  nm). Thus, this method is well suited to obtain additive manufactured optics with an appropriate surface quality. Nevertheless, this method is not the ideal solution for post-processing of the optics. First, the polishing process time does not fit to the philosophy of a rapid manufacturing process. When the additive manufacturing of the optical component requires <1 h, the post-processing method should not take longer. Second, additive manufacturing allows the generation of complex 3D shapes, which cannot be reworked by robots due to accessibility issues (e.g. undercuts).

Other solutions for post-treatment include chemical processes or coating processes. Thereby, the post-processing method must be adapted to the additive manufacturing process and to the polymer used. An example would be the chemical treatment of ABS polymer (FDM process) in a tempered acetone steam. This procedure leads to a significantly smoother surface. However, this method is of limited use for resins like in the case of the SLA process, and this method is often unsuitable for MJM materials. An alternative procedure is the coating of printed components. Thereby, it is important to note that the refractive index of the coating material should be

adapted to the refractive index of the additive material. In addition, the wettability of the polymer or the free energy of the polymer surface plays a crucial role. Suitable coating materials are varnishes or resins. Common techniques used are dip coating, spray coating, or spin coating. Ultimately, one needs to build up an appropriate material and process database.

Figure 5D shows an untreated 3d-printed lens (MJM method). As the inset reveals, the characteristic ring structures on the surface of the lens can be seen (the principal plane of the lens was parallel to the printing platform). The reflections of the overhead lights are hard to detect. In Figure 5E, the lens can be seen after a coating with a modified epoxy (spin coating). The surface structures are gone, and the overhead lights are clearly visible. Typical roughness values are around some 10 nm – depending on the printing method/polymer, coating material, and finishing process employed.

## 4 Selected examples for additive-manufactured optical components

This chapter should point out the potential of additive-manufactured optical components in various examples. The first example is the development of a borehole sensor [8]. The operating principle is demonstrated by the optical design (Figure 6A). Light from a laser diode is pointed directly to the additive-manufactured optical

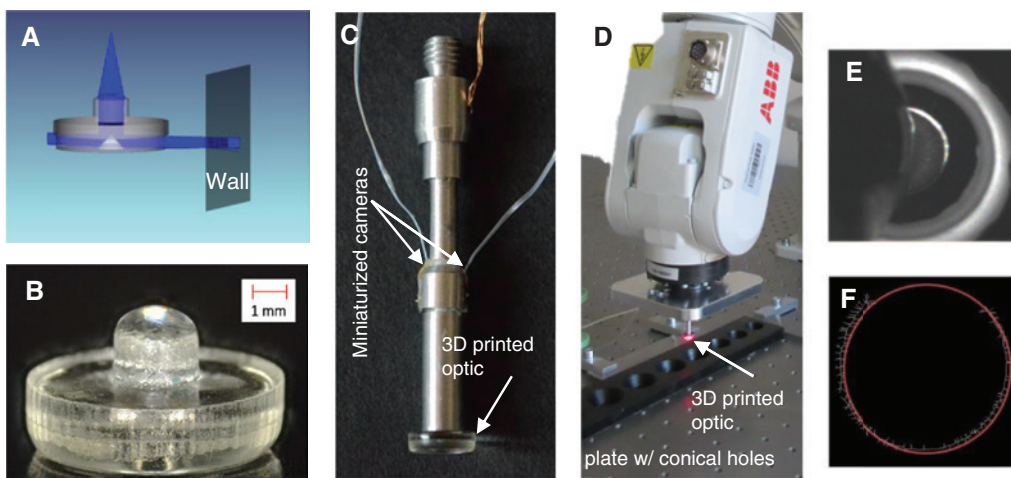


**Figure 6:** Bore hole sensor: (A) optic design; (B) 3d-printed optics; (C) sensor setup; (D) sensor mounted on robot; (E) image of a conical bore hole; (F) image processing.

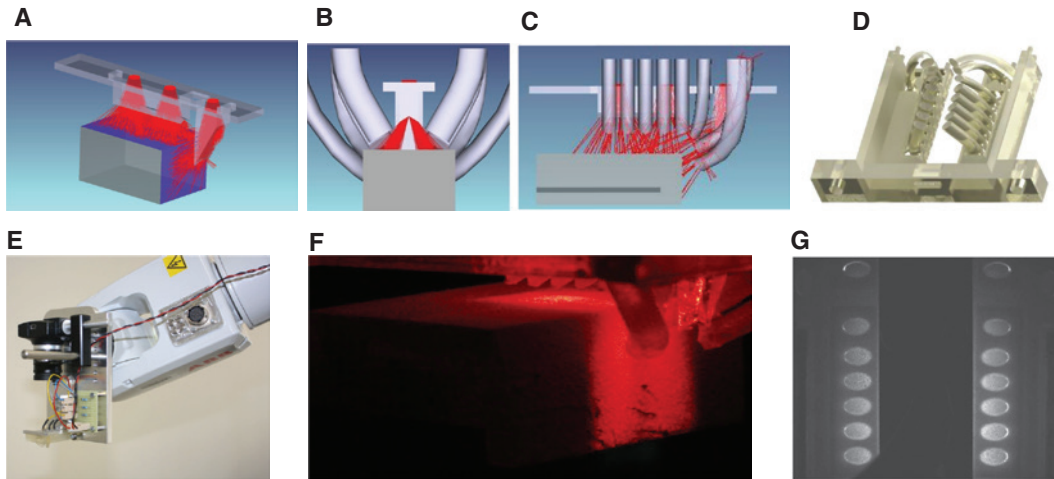


**Figure 7:** Tilt and surface damage sensor (A–C) basic principle; (D) 3d-printed detection unit (two light pipe rows); (E) integration of the sensor onto the robot; (F) measurement of a cubical part; (G) measurement result.

component from above. First, the laser beam is collimated by an aspherical surface and directed toward a conical structure. The cone is realized as a cavity within the material. Owing to the difference in refractive index between the optical component and air at the cavity surface, total internal reflection takes place, and light is reflected as a horizontal propagating ring. When light hits the (sufficiently rough) borehole wall, it is scattered in the entire hemisphere. If one arranges a camera above the optical component, the borehole wall can be recorded as a bright circle. This circle can be evaluated by means of image-processing software (e.g. with respect to diameter, waviness, etc.). Figure 6B shows the not reworked printed optical component or Figure 6C, the whole sensor setup. Thereby, two miniaturized cameras ( $1 \times 1 \times 1.4 \text{ mm}^3$ ) are integrated in the sensor element, so that the complete sensor can be immersed into the measurement object. The light source is located within the shaft. To move the sensor into the component, a robot is used (Figure 6D). Figure 6E shows a typical recording of one of the two miniaturized cameras. As conical holes have been measured in this case, a comparatively broad scan signal at the borehole wall can be seen (white circle). This signal is evaluated automatically by a MATLAB Software at a particular position of the sensor (represented by the robot coordinate) to determine the diameter of the hole at a certain z-position (see Figure 6F).

The realization of a sensor for in-line measurement of surface inclinations and surface defects is shown in Figure 7. The sensor is built up by an additive-manufactured illumination unit (including three laser diodes) (Figure 7A) and an additive-manufactured detection unit (Figure 7B–D). The lighting unit has the task to illuminate

two sides of a component (e.g. a cuboid) homogeneously. This demonstrates a significant advantage of additive manufacturing – the lighting design can be easily customized in order to fit the individual shape of the component. The detection unit consists of a series of light pipes, which direct the scattered light of the component surface ‘upward’ into the detection plane, where it is recorded by a camera. Thereby, the light pipes are arranged in two rows symmetrically with respect to the illumination axis (see Figure 7B and C). In the case that the object to be examined is parallel to the illumination or detection plane (see Figure 7B), both light pipe rows detect an identical signal. However, if the surface of the object is tilted (e.g. due to deformation or inclination of the component), one light pipe row measures an increased, the other one a decreased, scattering signal. After an initial referencing, the inclination or deformation can be deduced from the difference in scattering signal strength. The 3d-printed detection unit is shown in Figure 7D. The complete sensor setup (camera, illumination, and detection unit) is integrated onto a robot (Figure 7E). In Figure 7F, a typical experiment is shown. A corner area of a cuboid is illuminated. A typical measurement result can be seen in Figure 7G. A closer look reveals that the left light pipe row records a weaker signal than the right light pipe row, which can be evaluated. Using this method, tilt angle or surface defects can be detected in the range of degrees. This does not only depend on the sensor but on the surface quality of the part as well. Certainly, this is not a highly accurate measurement, but the design can be easily adapted individually for each measurement task and is sufficient for numerous fast machine vision applications.

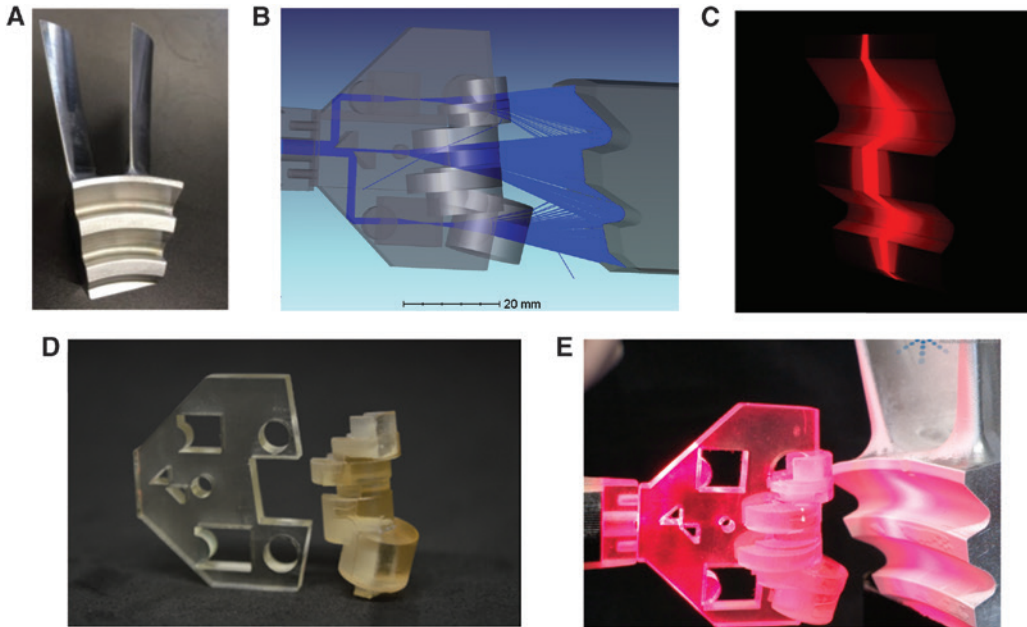


**Figure 8:** (A) Object to be examined; (B) optic design (LightTools, Synopsys, USA); (C) photorealistic rendering; (D) 3d-printed optical components; (E) experimental setup.

Another example for the use of additive-manufactured optics in the field of optical metrology is shown in Figure 8 [9, 10]. Figure 8A presents the object to be examined – the fir tree of a turbine blade. The task is to project a line like in the case of a laser triangulation sensor, but without any shadows on the part as this would lead to areas where the shape of the part cannot be measured. Thus, the projected line needs to follow the complex shape of the part. In this case, as a light source, a point-shaped laser beam is intended. Figure 8B shows a corresponding optical design. The light coming from the left is split via total internal reflecting surfaces into three beams. By cylindrical lens elements, a widening of the beams is gained. In addition, there are further tilted lens elements in the optical path, which ensure a shadow-free illumination of the surface. In Figure 8C, a photorealistic rendering reveals the expected line on the component (simulated in LightTools). Figure 8D shows the printed optics, which was divided into two sub-components in order to take the characteristics of the printer into account. In Figure 8E, an illumination experiment is shown – the generated line on the fir tree is comparable to the simulation (Figure 8C).

However, the example in Figure 8 also reveals that the received line compared with conventional laser triangulation sensor is quite broad. For an optimized spatial resolution, it would be better to generate a narrower line. For this purpose, investigations were carried out with different configurations of light pipes. An example is shown

in Figure 9. As seen in Figure 9A, the light pipe is completely surrounded by support material (white material). The light of a green laser is first pointed centrally onto the light pipe. Using a CCD camera,  $90^\circ$  deflected, at the front side of the pipe, emitted light is detected. As expected over the entire cross section of the pipe, scattered light is observed (Figure 9B). If the laser is pointed toward the interface region light pipe/support material, the light extraction at the front face of the light pipe changes significantly (Figure 9C, D). The resulting signal is a narrow line as the light is guided only along the interface layer. This effect looks similar to the light-guiding effect in an optical fiber.

Another possibility to generate a thin line is to use the intrinsic properties of the 3d-printing process. As shown in Figure 1B, the individual printed layers can be seen looking at the side face of a printed part. This also applies to the case of a cube. Looking at the top surface of a printed and untreated cube, no characteristic structure can be determined (Figure 10A). If a laser beam is coupled perpendicular to this surface, a diffuse spot due to the scattering within the material is generated (Figure 8B); edge length of the cube: 5 mm; spot measured at a distance of 60 cm). Investigating the side face of the cube (Figure 10C), the layered structure is detected (sine-shaped surface structure). If light is coupled perpendicular to this surface, a clear expansion of the laser beam in one direction appears (Figure 8D – signal measured at 60 cm distance). The sine-shaped structure acts like cylindrical

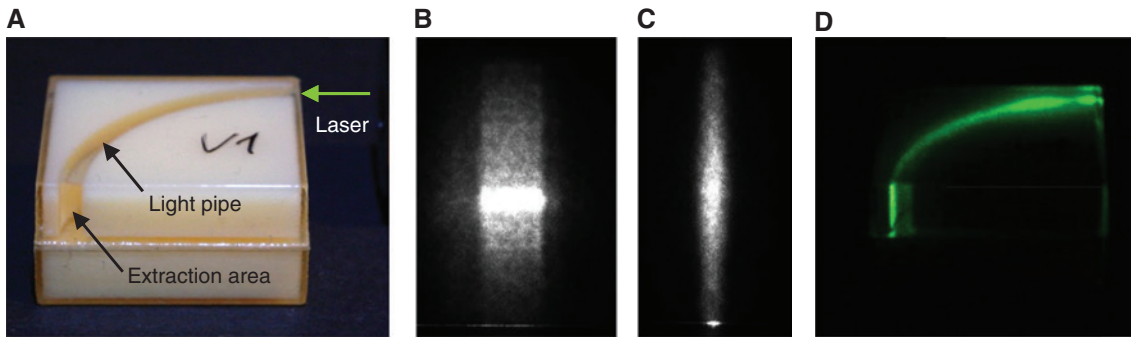


**Figure 9:** (A) Printed light pipe that is surrounded by support material (white); (B) image of the light extraction at the front surface of the light pipe – the laser light was coupled centrally into the pipe; (C) image of the light extraction at the front surface of the light pipe – the laser light was coupled at the interface building material/support material; (D) light guiding along the interface.

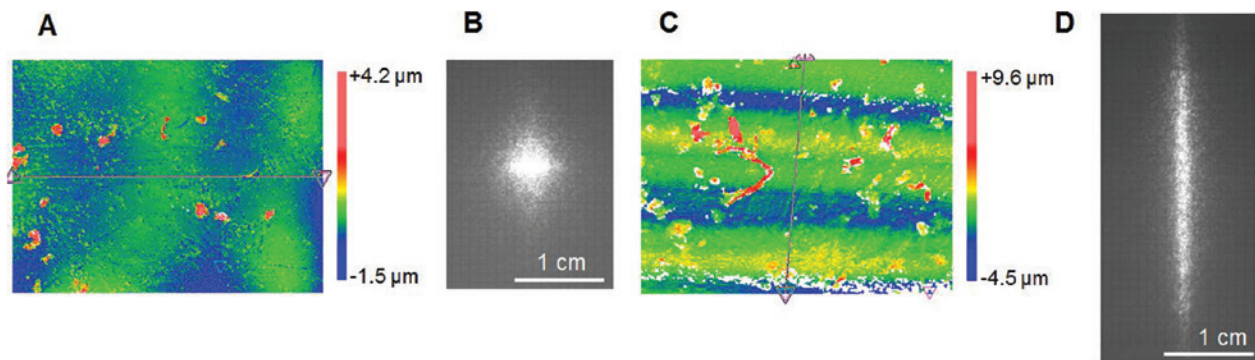


**Figure 10:** (A) surface topography (white light interferometer) of an untreated 3d-printed cube (top surface). (B) spot generated by a laser beam perpendicular to the top surface (distance: 60 cm); (C) surface topography of an untreated 3d-printed cube (side face); (D) spot generated by a laser beam perpendicular to the side face (distance: 60 cm).

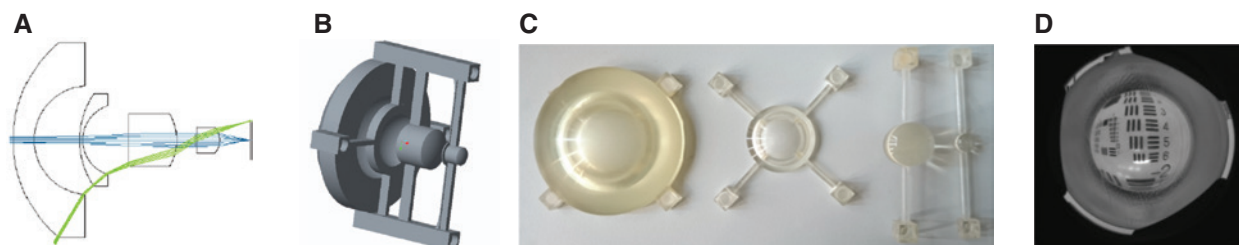


**Figure 11:** (A) Optic design fisheye; (B) opto-mechanic model; (C) 3d-printed lenses; (D) recorded MTF chart.

lens elements leading to the broadening of the beam in one direction.

So far, we have discussed the application of additive manufacturing for illumination optics. Finally, the question should be answered, whether this technology can be used for imaging optics as well. In order to do so, a fisheye lens was designed (Figure 11A). The design is based on a four-lens system. In addition to the designed optical elements, mechanical connections were added. In this way, the individual lenses can be assembled with

together without additional components (Figure 11B). The printed lens elements with their mechanical connections are shown in Figure 11C. A recorded MTF Chart for lens qualification is presented in Figure 11D. Basically, the experiments show that imaging optics can be realized with additive-manufactured components. However, their quality is significantly behind the conventionally produced imaging optics. Challenging topics are the tighter specifications for imaging optics (e.g. with regard to surface quality and transmission). Additionally compensating

chromatic effects (e.g. by an apochromat design) is not possible at this moment, as this would require adequate materials. The use of 3d printing for optical imaging does only make sense if new design approaches are needed. One example would be the inclusion of optically active structures in solid optical components, which cannot be realized with conventional methods.

## 5 Conclusions

In this work, different manufacturing techniques for the additive manufacturing of optical components were briefly introduced and compared. An important point was to show the boundaries of additive manufacturing of optical components. In addition to the transmission properties, the rework of the surface is crucial. For this purpose, robot-based polishing methods were used, but significantly shorter processing times are realized by applying chemical methods or by coating the printed parts. However, there is the challenge of finding the right coating material and the appropriate coating process for each printing technique and printing material. Furthermore, this paper describes the different examples of additive-manufactured optical components. Especially in the field of illumination optics, additive manufacturing technologies can contribute significantly. Thereby, the intrinsic properties of the 3d-printing process can be used in this purpose. A major challenge for imaging optics will be to improve the optical properties of the materials. For this purpose, open 3d-printing systems with a user free choice of materials and process parameters are needed to be able to adapt the manufacturing to the personal needs.

**Acknowledgments:** The authors wish to thank the support from German Federal Ministry of Education and Research, program 'FHProfUnt' (IMiSens, grant no. 03FH048PA4).

## References

- [1] R. Lachmayer, A. Wolf and G. Kloppenburg, SPIE Newsroom, 10.1117/2.1201511.006233 (2015).
- [2] R. Lachmayer, G. Kloppenburg and A. Wolf, Proc. SPIE 9383, 10.1117/12.2078791 (2015).
- [3] J. Klein, M. Stern, G. Franchin, M. Kayser, C. Inamura, et al., 2, 92–105, (M. A. Liebert Publishers, 2015).
- [4] T. Bückmann, M. Thiel, M. Kadic, R. Schittny and M. Wegener, Nat. Commun. 5, Article no.: 4130, doi: 10.1038/ncomms5130 (2014).
- [5] U. Berger, A. Hartmann and D. Schmid, in 'Additive Fertigungsverfahren Rapid Prototyping, Rapid Tooling, Rapid Manufacturing', (Verlag Europa-Lehrmittel, Nourney, Vollmer, Haan-Gruiten, 2013).
- [6] Wacker Feature Service, No. 1, 'Drucken mit Silicon' (2015).
- [7] ZPrinter Projet, 3D Systems.
- [8] A. Heinrich, B. Sorg, A. Grzesiak and U. Berger, Proc. DGAO annual meeting, Brno (2015).
- [9] A. Heinrich, P. Maillard, A. Suckow, A. Grzesiak, B. Sorg, et al., Proc. SPIE 9525, 10.1117/12.2183168 (2015).
- [10] P. Maillard and A. Heinrich, Proc. SPIE 9628, 10.1117/12.2191280 (2015).



**Andreas Heinrich**  
Center for Optical Technologies  
Aalen University, Anton Huber Straße  
21, 73430 Aalen, Germany  
[Andreas.Heinrich@hs-aalen.de](mailto:Andreas.Heinrich@hs-aalen.de)

Andreas Heinrich received his Diploma in Physics and his PhD from the Technical University Munich in 1998 and 2001, respectively. In 2001, he joined the University Augsburg as a research fellow and completed his Habilitation in 2006. From 2007 to 2013, he worked at Carl Zeiss. His current position is professor at the Hochschule Aalen and head of the optical metrology group at the Center for Optical Technologies.

**Manuel Rank**  
Center for Optical Technologies, Aalen University, Anton Huber Straße 21, 73430 Aalen, Germany

Manuel Rank studied Opto-electronics and Photonics at the University of Applied Science Aalen. Currently he is doing his PhD at the optical metrology group in the field of additive manufacturing of optical components.

**Anne Suckow**  
Center for Optical Technologies, Aalen University, Anton Huber Straße 21, 73430 Aalen, Germany

Anne Suckow studied Optometry and Vision Science at the University of Applied Science Jena. Since 2015 she is a scientific assistant in the field of additive manufacturing of optics at the optical metrology group, Center for Optical Technologies.

**Philippe Maillard, Yannick Bauckhage, Patrick Rößler, Johannes Lang, Fatin Shariff and Sven Pekrul**  
Center for Optical Technologies, Aalen University, Anton Huber Straße 21, 73430 Aalen, Germany

Philippe Maillard, Yannick Bauckhage, Patrick Rößler, Johannes Lang, Fatin Shariff and Sven Pekrul are students of the optical metrology group and are doing their Bachelor or Master Thesis in the field of additive manufactured optics.